

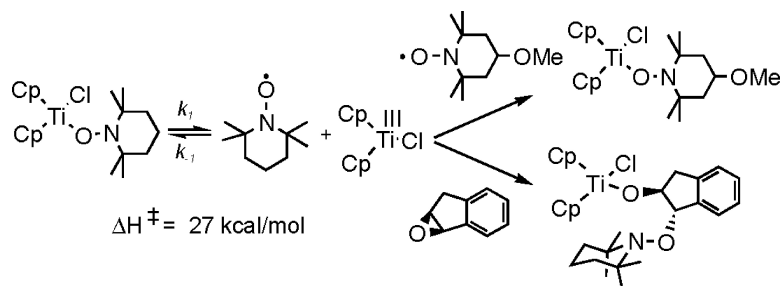
Article

Homolysis of Weak Ti–O Bonds: Experimental and Theoretical Studies of Titanium Oxygen Bonds Derived from Stable Nitroxyl Radicals

Kuo-Wei Huang, Joseph H. Han, Adam P. Cole, Charles B. Musgrave, and Robert M. Waymouth

J. Am. Chem. Soc., **2005**, 127 (11), 3807-3816 • DOI: 10.1021/ja044512f • Publication Date (Web): 25 February 2005

Downloaded from <http://pubs.acs.org> on March 24, 2009



More About This Article

Additional resources and features associated with this article are available within the HTML version:

- Supporting Information
- Links to the 2 articles that cite this article, as of the time of this article download
- Access to high resolution figures
- Links to articles and content related to this article
- Copyright permission to reproduce figures and/or text from this article

[View the Full Text HTML](#)

Homolysis of Weak Ti–O Bonds: Experimental and Theoretical Studies of Titanium Oxygen Bonds Derived from Stable Nitroxyl Radicals

Kuo-Wei Huang,[†] Joseph H. Han,[‡] Adam P. Cole,[†] Charles B. Musgrave,^{‡,§} and Robert M. Waymouth^{*,†,‡}

Contribution from the Departments of Chemistry, Chemical Engineering, and Materials Science and Engineering, Stanford University, Stanford, California 94305

Received September 10, 2004; E-mail: waymouth@stanford.edu

Abstract: Titanium–oxygen bonds derived from stable nitroxyl radicals are remarkably weak and can be homolyzed at 60 °C. The strength of these bonds depends sensitively on the ancillary ligation at titanium. Direct measurements of the rate of Ti–O bond homolysis in Ti–TEMPO complexes Cp₂TiCl(TEMPO) (**3**) and Cp₂TiCl(4-MeO-TEMPO) (**4**) (TEMPO = 2,2,6,6-tetramethylpiperidine-*N*-oxyl, 4-MeO-TEMPO = 2,2,6,6-tetramethyl-4-methoxypiperidine-*N*-oxyl) were conducted by nitroxyl radical exchange experiments. Eyring plots gave the activation parameters, $\Delta H^\ddagger = 27(\pm 1)$ kcal/mol, $\Delta S^\ddagger = 6.9(\pm 2.3)$ eu for **3** and $\Delta H^\ddagger = 28(\pm 1)$ kcal/mol, $\Delta S^\ddagger = 9.0(\pm 3.0)$ eu for **4**, consistent with a process involving the homolysis of a weak Ti–O bond to generate the transient Cp₂Ti(III)Cl and the nitroxyl radical. Thermolysis of the titanocene TEMPO complexes in the presence of epoxides leads to the Cp₂Ti(III)Cl-mediated ring-opening of the epoxide followed by trapping by the nitroxyl radical. The X-ray crystal structure of the Ti–TEMPO derivative, Cp₂TiCl(4-MeO-TEMPO) (**4**), is reported. DFT (B3LYP/6-31G*) calculations and experimental studies reveal that the strength of the Ti–O bond decreases dramatically with the number of cyclopentadienyl groups on titanium. The calculated Ti–O bond strength of the monocyclopentadienyl complex **2** is 43 kcal/mol, whereas that of the biscyclopentadienyl complex **3** is 17 kcal/mol, a difference of 26 kcal/mol. These studies reveal that the strength of these Ti–O bonds can be tuned over an interesting and experimentally accessible temperature range by appropriate ligation on titanium.

Introduction

Transition-metal radicals have a rich reaction chemistry that is often distinct from their diamagnetic congeners.¹ Odd-electron organometallic complexes derived from low-valent transition metals have proven to be useful for a variety of organic transformations;^{2–5} those from Ti(III), in particular, have engendered interest for their utility in regioselective epoxide opening and pinacol couplings.^{5–10} As part of our interest in the chemistry of Ti(III) polymerization catalysts,¹¹ we initiated studies to develop a general strategy for generating Ti(III) complexes from the homolysis of weak metal–ligand covalent

bonds derived from stable radicals, in analogy to approaches utilized in living free-radical polymerization.^{12–14} This approach requires metal–ligand bonds of the appropriate energy to be homolyzed thermally, and for this reason, we were attracted to the stable nitroxyl radical TEMPO (2,2,6,6-tetramethylpiperidine-1-oxyl).

At the onset of our studies, little was known of the coordination chemistry or bonding energetics of stable nitroxyl radicals to early metals.^{15–17} We have shown that the coordination chemistry of hydroxylaminate ligands (i.e., those derived from nitroxyl radicals or hydroxylamines) depends sensitively on the ligation environment of titanium.^{18–21} In the absence of other sterically demanding ligands, the hydroxyl-derived ligand

[†] Department of Chemistry.

[‡] Department of Chemical Engineering.

[§] Department of Materials Science and Engineering.

- (1) Astruc, D. *Electron Transfer Processes in Transition-Metal Chemistry*; Wiley-VCH: New York, 1995.
- (2) Skrydstrup, T. *Angew. Chem., Int. Ed. Engl.* **1997**, *36*, 345–347.
- (3) Molander, G. A.; Harris, C. R. *Tetrahedron* **1998**, *54*, 3321–3354.
- (4) Gansauer, A.; Lauterbach, T.; Bluhm, H.; Noltemeyer, M. *Angew. Chem., Int. Ed.* **1999**, *38*, 2909–2910.
- (5) Spencer, R. P.; Schwartz, J. *Tetrahedron* **2000**, *56*, 2103–2112.
- (6) Rajanbabu, T. V.; Nugent, W. A. *J. Am. Chem. Soc.* **1994**, *116*, 986–997.
- (7) Gansauer, A.; Bluhm, H. *Chem. Rev.* **2000**, *100*, 2771–2788.
- (8) Gansauer, A.; Pierobon, M.; Bluhm, H. *Synthesis* **2001**, 2500–2520.
- (9) Gansauer, A.; Bluhm, H.; Rinker, B.; Narayan, S.; Schick, M.; Lauterbach, T.; Pierobon, M. *Chem.–Eur. J.* **2003**, *9*, 531–542.
- (10) Gansauer, A.; Rinker, B. In *Titanium and Zirconium in Organic Synthesis*; Marek, I., Ed.; Wiley-VCH: Weinheim, Germany, 2002; pp 435–450.
- (11) Mahanthappa, M. K.; Waymouth, R. M. *J. Am. Chem. Soc.* **2001**, *123*, 12093–12094.

- (12) Benoit, D.; Harth, E.; Fox, P.; Waymouth, R. M.; Hawker, C. J. *Macromolecules* **2000**, *33*, 363–370.
- (13) Marque, S.; Le Mercier, C.; Tordo, P.; Fischer, H. *Macromolecules* **2000**, *33*, 4403–4410.
- (14) Hawker, C. J.; Bosman, A. W.; Harth, E. *Chem. Rev.* **2001**, *101*, 3661–3688.
- (15) Golubev, V. A.; Voronina, G. N.; Chernaya, L. I.; Dyachkovskii, F. S.; Matkovskii, P. E. *Zh. Obshch. Khim.* **1977**, *47*, 1825–1832.
- (16) Brindley, P. B.; Scotton, M. J. *J. Organomet. Chem.* **1981**, *222*, 89–96.
- (17) Evans, W. J.; Perotti, J. M.; Doedens, R. J.; Ziller, J. W. *Chem. Commun.* **2001**, 2326–2327.
- (18) Huang, K.-W.; Waymouth, R. M. *J. Am. Chem. Soc.* **2002**, *124*, 8200–8201.
- (19) Mahanthappa, M. K.; Huang, K.-W.; Cole, A. P.; Waymouth, R. M. *Chem. Commun.* **2002**, 502–503.
- (20) Mahanthappa, M. K.; Cole, A. P.; Waymouth, R. M. *Organometallics* **2004**, *23*, 836–845.

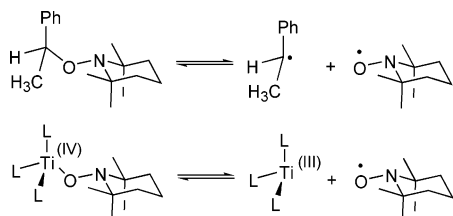


Figure 1. Homolysis of Ti–O bonds derived from stable radicals.

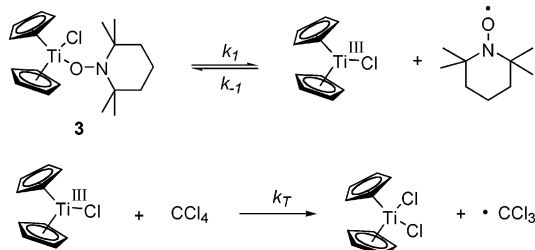


Figure 2. Thermolysis of titanium TEMPO complexes in CCl_4 .

TEMPO adopts an η^2 -coordination geometry for $\text{Cl}_3\text{Ti}(\text{TEMPO})$ **1** in the solid state, but in solution, the TEMPO ligand is labile and undergoes an η^1 – η^2 interconversion.²¹ The presence of cyclopentadienyl ligands enforces an η^1 -coordination geometry on the TEMPO ligand for $\text{CpTiCl}_2(\text{TEMPO})$ **2**.¹⁹

The thermal stability of the cyclopentadienyl titanium TEMPO complexes $\text{CpTiCl}_2(\text{TEMPO})$ **2** and $\text{Cp}_2\text{TiCl}(\text{TEMPO})$ **3** depends sensitively on the number of cyclopentadienyl groups on titanium; complex **2** was stable for days at 100 °C in CCl_4 , whereas the TEMPO ligand is exchanged for chloride upon thermolysis of **3** in CCl_4 (Figure 2).¹⁸

Mechanistic studies provided evidence for the homolytic cleavage of a weak Ti–O bond of **3**.¹⁸ The facile homolysis of the Ti–O bond of **3** is indicative of a remarkably weak Ti–O bond, consistent with our hypothesis that Ti–O bonds derived from stable radicals should be much weaker than those derived from alkoxides (approximately 90 kcal/mol).²² What we had not anticipated was the dramatic influence of the cyclopentadienyl ligands on the strength of these Ti–O bonds; the fact that **2** is thermally stable at 100 °C for extended periods suggests that the strength of these Ti–O bonds might be tunable over an interesting and experimentally accessible temperature range by appropriate manipulation of the ligand environment at titanium. In this paper, we report experimental studies on the homolysis of weak Ti–O bonds derived from stable radicals combined with theoretical studies to assess how the strength of these bonds can be tuned by appropriate choice of the ligand environment or nature of the nitroxyl radical.

Results and Discussion

To investigate the role of ligand effects on the bonding geometry and energetics of this family of compounds, we prepared a series of titanium hydroxylaminate compounds **1–5** (Figure 3). The synthesis was carried out by reduction of a suitable Ti(IV) halide precursor, followed by trapping of the Ti(III) intermediate with the nitroxyl radical.^{18,19}

(21) Mahanthappa, M. K.; Cole, A. P.; Waymouth, R. M. *Organometallics* **2004**, *23*, 1405–1410.

(22) Calhorda, M. J.; Carrondo, M. A. F. D. C. T.; Dias, A. R.; Domingos, A. M. T. S.; Simoes, J. A. M.; Teixeira, C. *Organometallics* **1986**, *5*, 660–667.

To investigate the structural effects of biscyclopentadienyl ligation on the TEMPO ligand, an X-ray structural study of **4** was carried out (**3** did not yield suitable crystals for an X-ray structure). Crystallization of **4** from pentane afforded thin brown plates suitable for X-ray crystallographic analysis. The structure of **4** reveals that 4-MeO-TEMPO coordinates to the titanium in an η^1 geometry (Figure 4). The Ti–O bond distance of 1.824 Å and the N–O bond distance of 1.406 Å are indicative of a reduced TEMPO ligand, as observed for **2**.¹⁹ Comparison of the bonding geometry of **4** relative to that of the monocyclopentadienyl compound **2** reveals several significant differences, notably, a longer Ti–O bond (1.824 Å for **4** versus 1.752 Å for **2**) and a smaller Ti–O–N bond angle (145.6° for **4** versus 155.7° for **2**).¹⁹ The longer Ti–O bonds for the biscyclopentadienyl derivative **4** (and **3**, vide infra) is consistent with trends observed for mono- and biscyclopentadienyl titanium alkoxides.^{23–26} This lengthening also correlates with our experimental observations that the Ti–O bond of **3** is more readily homolyzed than that of **2**. The Ti–O–N angle of **4** is similar to that observed in other titanocene alkoxides and sulfides.^{23,27,28} The smaller Ti–O–N angle of **4** relative to that of **2** may be indicative of reduced p_π to d_π donation from the oxygen to the titanium center upon substitution by the second cyclopentadienyl ligand,^{23–25} although as pointed out by Parkin and Rothwell,^{28,29} M–O–R angles are not predictive indicators of the degree of π -donation in early metal alkoxides.

To provide further evidence for the homolytic Ti–O bond cleavage of **3** and to provide an experimental estimate of the Ti–O bond strengths of the biscyclopentadienyl complexes **3–5**, we investigated the kinetics of Ti–O bond homolysis by nitroxyl exchange experiments. Previous studies on the thermolysis of **3** in the presence of carbon tetrachloride (Figure 2) revealed that the coupling of nitroxyl radical with Cp_2TiCl (**8**) was much faster than chlorine atom abstraction from CCl_4 ,³⁰ which precluded a direct measurement of the rate of Ti–O bond homolysis.¹⁸ Among other possible trapping reagents for Ti(III) (such as CBr_4), we found that nitroxyl radicals underwent clean exchange reactions that could be readily monitored by ¹H NMR (Figure 5).

The thermolysis of **3** in the presence of excess 4-MeO-TEMPO (**10**) was monitored by ¹H NMR.³¹ Initial rates were monitored as the system approached equilibrium at high conversion. Plots of $\ln([\mathbf{3}]_0/[\mathbf{3}]_t)$ versus time were linear with a zero intercept; a plot of the pseudo-first-order rate constant k_{obs} versus [4-MeO-TEMPO] (= [**10**]₀) at 60 °C in d_6 -benzene indicated that the rates were zero order in nitroxyl **10**. Monitor-

(23) Kalirai, B. S.; Foulon, J. D.; Hamor, T. A.; Jones, C. J.; Beer, P. D.; Fricker, S. P. *Polyhedron* **1991**, *10*, 1847–1856.

(24) Thorn, M. G.; Vilaro, J. S.; Lee, J.; Hanna, B.; Fanwick, P. E.; Rothwell, I. P. *Organometallics* **2000**, *19*, 5636–5642.

(25) Nomura, K.; Naga, N.; Miki, M.; Yanagi, K. *Macromolecules* **1998**, *31*, 7588–7597.

(26) Huffman, J. C.; Moloy, K. G.; Marsella, J. A.; Caulton, K. G. *J. Am. Chem. Soc.* **1980**, *102*, 3009–3014.

(27) Calhorda, M. J.; Carrondo, M. A. F. D. T.; Dias, A. R.; Frazao, C. F.; Hursthouse, M. B.; Simoes, J. A. M.; Teixeira, C. *Inorg. Chem.* **1988**, *27*, 2513–2518.

(28) Howard, W. A.; Trnka, T. M.; Parkin, G. *Inorg. Chem.* **1995**, *34*, 5900–5909.

(29) Coffindaffer, T. W.; Rothwell, I. P.; Huffman, J. C. *Inorg. Chem.* **1983**, *22*, 2906–2910.

(30) Tenhaeff, S. C.; Covert, K. J.; Castellani, M. P.; Grunkemeier, J.; Kunz, C.; Weakley, T. J. R.; Koenig, T.; Tyler, D. R. *Organometallics* **1993**, *12*, 5000–5004.

(31) Budzelaar, P. H. M. *gNMR*, version 4.1; Adept Scientific, Herts, (www.adeptscience.com); Cherwell Scientific Publishing: 1999.

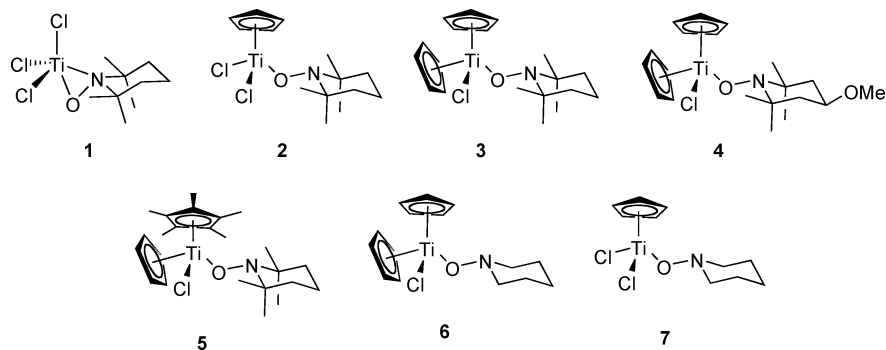


Figure 3. Titanium hydroxylaminato complexes.

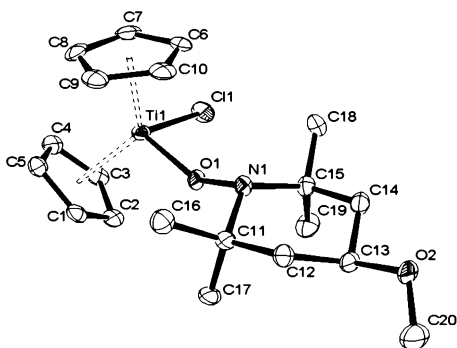


Figure 4. ORTEP drawing of **4**. Selected bond distances (Å) and angles (deg): Ti1–O1, 1.824(2); Ti1–Cl1, 2.5346(12); N1–O1, 1.406(3); Cp1–Ti, 2.019; Cp2–Ti, 2.028; C11–Ti1–O1, 98.00(8); Ti1–O1–N1, 145.64(19); O1–N1–C11, 109.1(2); O1–N1–C15, 103.8(2); C11–N1–C15, 120.4(3); Cp1–Ti–Cp2, 127.0.

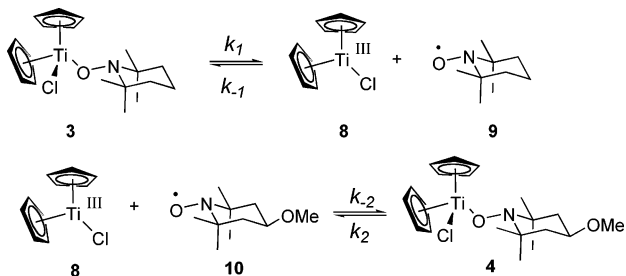


Figure 5. Nitroxyl radical exchange.

ing the initial rates under conditions where $k_{-2}[\mathbf{10}]_0 \gg k_{-1}[\mathbf{9}]$ yields an estimate of k_1 , the rate constant for Ti–O bond homolysis (eq 1).

$$\text{rate} = -\frac{d[\mathbf{3}]}{dt} = \left(\frac{k_{-2}[\mathbf{10}]}{k_{-1}[\mathbf{9}] + k_{-2}[\mathbf{10}]} \right) k_1[\mathbf{3}] \quad (1)$$

The rate constants of Ti–O homolysis of **3** and **4** in d_6 -benzene at different temperatures (40–65 °C) were measured (Table 1). The thermolysis of **4** was carried out under similar conditions with TEMPO as the nitroxyl radical. These experiments revealed that k_{obs} for the homolysis of **4** was approximately one-half that of **3**. The enthalpies of activation for bond homolysis reactions are related to the bond dissociation energies^{32–38} and were obtained from Eyring plots of $\ln(kh/$

Table 1. Value of k_{obs} for the Thermolysis of **3** and **4** in the Presence of Nitroxyl Radicals^a

entry	$[\mathbf{10}]_0$ (M)	$[\mathbf{9}]_0$ (M)	T (°C)	k_{obs} (10^{-4} s^{-1})
1 ^b	0.100		60	9.3 ± 1.0
2 ^b	0.150		60	9.3 ± 0.5
3 ^b	0.200		60	9.3 ± 0.7
4 ^b	0.250		60	10 ± 1
5 ^b	0.200		40	0.63 ± 0.11
6 ^b	0.200		45	1.4 ± 0.2
7 ^b	0.200		50	2.9 ± 0.8
8 ^b	0.200		55	4.7 ± 0.4
9 ^b	0.200		65	17 ± 2
10 ^c		0.200	40	0.32 ± 0.05
11 ^c		0.200	50	1.2 ± 0.2
12 ^c		0.200	60	4.2 ± 0.5
13 ^c		0.200	65	9.7 ± 1.3

^a $[\mathbf{3}]_0 = 1.0 \times 10^{-2} \text{ M}$, $[\mathbf{4}]_0 = 1.0 \times 10^{-2} \text{ M}$. ^b Plotting $\ln([\mathbf{3}]_0/[\mathbf{3}]_t)$ vs time. ^c Plotting $\ln([\mathbf{4}]_0/[\mathbf{4}]_t)$ vs time.

$k_{\text{B}}T$) versus $1/T$ (k = rate constant; h = Planck constant; k_{B} = Boltzmann constant; T in Kelvin). The kinetics and activation parameters, $\Delta H^\ddagger = 27(\pm 1) \text{ kcal/mol}$, $\Delta S^\ddagger = 6.9(\pm 2.3) \text{ eu}$ ($\Delta G^\ddagger = 24.2 \text{ kcal/mol}$ at 60 °C) for **3** and $\Delta H^\ddagger = 28(\pm 1) \text{ kcal/mol}$, $\Delta S^\ddagger = 9.0(\pm 3.0) \text{ eu}$ ($\Delta G^\ddagger = 24.7 \text{ kcal/mol}$ at 60 °C) for **4**, are consistent with those of a process involving the homolysis of a weak Ti–O bond and are comparable to those obtained for the homolysis of cobalt–carbon bonds within a similar temperature range.^{32,33,35,39} Accounting for possible contributions from cage effects^{37,38,40–42} places an upper-limit of the Ti–O bond dissociation energy of **3** of approximately 25 kcal/mol, which constitutes the weakest Ti–O bond known for neutral complexes.^{22,43,44} The slower rate of homolysis of **4** relative to that of **3** indicates that the activation energies of Ti–O homolysis reactions depend on the nature of the nitroxyl radical, as observed for the homolysis of organic alkoxyamines.^{13,45}

Equilibrium measurements with known concentrations of **3**, **9**, **4**, and **10** yielded an equilibrium constant for nitroxyl radical exchange, $K = ([\mathbf{4}][\mathbf{9}]/[\mathbf{3}][\mathbf{10}]) = 2.0 \pm 0.2$ (Table 2). These

(32) Halpern, J. *Polyhedron* **1988**, *7*, 1483–1490 and references therein.

(33) Halpern, J. *Bull. Chem. Soc. Jpn.* **1988**, *61*, 13–15.

(34) Daikh, B. E.; Finke, R. G. *J. Am. Chem. Soc.* **1992**, *114*, 2938–2943.

(35) Brown, K. L.; Zhou, L. *Inorg. Chem.* **1996**, *35*, 5032–5039.

(36) Hay, B. P.; Finke, R. G. *Polyhedron* **1988**, *7*, 1469–1481 and references therein.

(37) Koenig, T.; Finke, R. G. *J. Am. Chem. Soc.* **1988**, *110*, 2657–2658.

(38) Koenig, T.; Hay, B. P.; Finke, R. G. *Polyhedron* **1988**, *7*, 1499–1516.

(39) Experimental considerations limited the temperature range (15 °C) over which the activation parameters could be measured, and thus some error can be expected in the Eyring analysis.

(40) Visanath, D. S.; Natarajan, G. *Data Book on the Viscosity of Liquids*; Hemisphere Publishing Corp.: New York, 1989.

(41) Braden, D. A.; Parrack, E. E.; Tyler, D. R. *Coord. Chem. Rev.* **2001**, *211*, 279–294.

(42) Male, J. L.; Lindfors, B. E.; Covert, K. J.; Tyler, D. R. *J. Am. Chem. Soc.* **1998**, *120*, 13176–13186.

(43) Schmittel, M.; Soellner, R. *Angew. Chem., Int. Ed. Engl.* **1996**, *35*, 2107–2109.

(44) Schmittel, M.; Burghart, A.; Werner, H.; Laubender, M.; Soellner, R. *J. Org. Chem.* **1999**, *64*, 3077–3085.

(45) Skene, W. G.; Belt, S. T.; Connolly, T. J.; Hahn, P.; Scaiano, J. C. *Macromolecules* **1998**, *31*, 9103–9105.

Table 2. Equilibrium at 60 °C^a

entry	[4] ₀ (M)	[10] ₀ (M)	[9] ₀ (M)	[3]/[4]	K
1	1.0 × 10 ⁻²	9.24 × 10 ⁻²	1.85 × 10 ⁻¹	1.1	1.7 ± 0.3
2	8.0 × 10 ⁻³	1.18 × 10 ⁻¹	1.07 × 10 ⁻¹	0.52	2.3 ± 0.3
3	2.4 × 10 ⁻²	6.56 × 10 ⁻²	2.08 × 10 ⁻¹	1.7	1.9 ± 0.3

^a Initial concentration of [3] = 0. The equilibrium was reached after 150 min at 60 °C.

experiments indicate that the Ti–O bond energy of **4** is greater than that of **3** by approximately 0.5 kcal/mol (assuming $\Delta S^\circ \approx 0$), comparable to the bond energy difference of C–O bonds between *N*-benzoxyl-2,2,6,6-tetramethylpiperidine and *N*-benzoxyl-4-hydroxyl-2,2,6,6-tetramethylpiperidine (30.8 versus 31.4 kcal/mol, respectively).⁴⁵

The influence of the nature of the cyclopentadienyl ligand was investigated by replacing one Cp ligand of **3** with a Cp* (pentamethylcyclopentadienyl) group.⁴⁶ The rate of thermolysis of Cp*CpTiCl(TEMPO) (**5**) in the presence of 4-MeO-TEMPO ($3.2(\pm 0.3) \times 10^{-3} \text{ s}^{-1}$ at 50 °C) was found to be 10 times greater than that of **2**. This result provides a further indication that the strength of these Ti–O bonds can be sensitively tuned through the choice of appropriate ancillary ligands.

These studies provide clear evidence that the homolysis of weak bonds derived from stable radicals provides a novel strategy for the generation of odd-electron Ti(III) organometallics. As Nugent and Gansauer have shown that Cp₂Ti(III)Cl is a powerful reagent for the ring-opening of epoxides,^{4–10} we investigated the reactivity of **3** with epoxides (Figure 6). Thermolysis of **3** in the presence of styrene oxide at 100 °C for 10 min in toluene yielded the titanocene alkoxyamine **12** in quantitative yield by ¹H NMR (72% isolated yield). Similarly, thermolysis of **3** in the presence of indene oxide **13** at 100 °C for 5 min yielded a single diastereomer of the titanocene alkoxyamine **14**, which could be hydrolyzed to the alkoxyamine **15** (94% isolated yield). The high diastereoselectivity of the latter process is intriguing and implies that the biscyclopentadienyl titanium fragment constrains the approach of the nitroxyl radical, yielding a highly diastereoselective coupling of the nitroxyl and benzyl radical fragments. Thus, ring-opening of epoxides by the titanocene TEMPO complex **3** provides a stereoselective strategy for the ring-opening of benzylic epoxides with the introduction of an alkoxyamine at the benzylic position which can be used for further elaboration. Aryl diols, such as 1,2-indanediols, are useful intermediates for agrochemical and pharmaceutical applications⁴⁷ and can be obtained from the enantioselective epoxidation of indene.^{48,49} Further studies on the scope and limitations of these radical epoxide opening reactions are in progress.

The facile trapping of the benzylic radical upon ring-opening of styrene oxide by TEMPO provided a further experimental protocol to measure the rate of Ti–O bond homolysis. The kinetics of the ring-opening of styrene oxide were measured at 60 °C in *d*₆-benzene under pseudo-first-order conditions with excess styrene oxide. Thermolysis of **3** in the presence of excess

styrene oxide yielded clean first-order kinetics out to four half-lives. The rate constant measured from these experiments at 60 °C in C₆D₆ toluene ($k_{\text{obs}} = 10.2(\pm 0.2) \times 10^{-4} \text{ s}^{-1}$) is in very good agreement with the rate of Ti–O bond homolysis measured from the initial rates in the nitroxyl exchange experiments (Table 1).⁵⁰ These studies reveal that under these conditions, the rate of trapping of the CpTi(III)Cl fragment **8** by styrene oxide is faster than that of the nitroxyl radical **9**, a consequence of the lower concentration of **9** engendered by its rapid reaction with the benzyl radical **16** (Figure 7).

DFT Calculations. The results of the nitroxide exchange and the epoxide ring-opening experiments provide clear evidence that homolysis of Ti–O bonds derived from stable nitroxyl radicals provides a novel strategy for generating Ti(III) intermediates. These studies reveal that these Ti–O bonds are considerably weaker than those of titanium alkoxides, at least for the biscyclopentadienyl derivatives **3** and **4**. However, the observation that the Ti–O bonds of monocyclopentadienyl complexes **2** are not readily homolyzed at 100 °C reveals that the strengths of these weak Ti–O bonds are sensitive to ancillary ligation at titanium. To investigate the influence of ancillary ligands on the bonding energetics of these Ti–O bonds, we carried out a series of DFT calculations using the Gaussian 98 program⁵¹ on complexes **1–4**, **6**, and **7**. To calibrate our method, we first surveyed a variety of DFT methods and basis sets and compared the optimized geometries of the calculated structures of **1** and **2** with X-ray crystal structures. On the basis of these studies, we found that the B3LYP^{52,53} gradient-corrected exchange hybrid DFT method combined with a 6-31G(d)^{54–57} basis set resulted in a good compromise of accuracy and computational expense. This hybrid functional has been shown to have relatively good accuracy at moderate computational cost and has been used previously to investigate titanium–oxygen bonds.^{57–59} This level of theory has been shown to underestimate the experimentally measured bond dissociation energies of organic alkoxyamines,⁶⁰ by approximately 7–8 kcal/mol; nevertheless, as we were most interested in the effects on ancillary ligands on the trends in the Ti–O bond energies, the B3LYP/6-31G* level of theory was judged adequate to provide an estimate of these trends.

Structural Simulations of Cl₃Ti(TEMPO) (1) and CpTiCl₂(TEMPO) (2). Three initial binding configurations of TEMPO

(50) See Supporting Information for the derivation of the rate law and figures giving a summary of the kinetic data.

- (51) Frisch, M. J.; Trucks, G. W.; Schlegel, H. B.; Scuseria, G. E.; Robb, M. A.; Cheeseman, J. R.; Zakrzewski, V. G.; Montgomery, J. A., Jr.; Stratmann, R. E.; Burant, J. C.; Dapprich, S.; Millam, J. M.; Daniels, A. D.; Kudin, K. N.; Strain, M. C.; Farkas, O.; Tomasi, J.; Barone, V.; Cossi, M.; Cammi, R.; Mennucci, B.; Pomelli, C.; Adamo, C.; Clifford, S.; Ochterski, J.; Petersson, G. A.; Ayala, P. Y.; Cui, Q.; Morokuma, K.; Rega, N.; Salvador, P.; Dannenberg, J. J.; Malick, D. K.; Rabuck, A. D.; Raghavachari, K.; Foresman, J. B.; Cioslowski, J.; Ortiz, J. V.; Baboul, A. G.; Stefanov, B. B.; Liu, G.; Liashenko, A.; Piskorz, P.; Komaromi, I.; Gomperts, R.; Martin, R. L.; Fox, D. J.; Keith, T.; Al-Laham, M. A.; Peng, C. Y.; Nanayakkara, A.; Challacombe, M.; Gill, P. M. W.; Johnson, B.; Chen, W.; Wong, M. W.; Andres, J. L.; Gonzalez, C.; Head-Gordon, M.; Replogle, E. S.; Pople, J. A., *Gaussian 98, Rev. A.11.2*; Gaussian, Inc.: Pittsburgh, PA, 2001.
- (52) Becke, A. J. *Chem. Phys.* **1993**, *98*, 5648–5652.
- (53) Lee, C.; Yang, W.; Parr, R. *Phys. Rev. B* **1988**, *37*, 785–789.
- (54) Ditchfield, R.; Hehre, W.; Pople, J. *J. Chem. Phys.* **1971**, *54*, 724–728.
- (55) Hehre, W.; Ditchfield, R.; Pople, J. *J. Chem. Phys.* **1972**, *56*, 2257–2261.
- (56) Hariharu, P.; Pople, J. *Theor. Chim. Acta* **1973**, *28*, 213–222.
- (57) Dobado, J. A.; Molina, J. M.; Ugglar, R.; Sundberg, M. R. *Inorg. Chem.* **2000**, *39*, 2831–2836.
- (58) Bergstrom, R.; Lunell, S.; Eriksson, L. *Int. J. Quantum Chem.* **1996**, *59*, 427–443.
- (59) Flisak, Z.; Szczegot, K. *J. Mol. Catal.* **2003**, *206*, 429–434.
- (60) Marsal, P.; Roche, M.; Tordo, P.; Claire, P. D. *J. Phys. Chem. A* **1999**, *103*, 2899–2905.

(46) Rogers, R. D.; Benning, M. M.; Kurihara, L. K.; Moriarty, K. J.; Rausch, M. D. *J. Organomet. Chem.* **1985**, *293*, 51–60.

(47) Page, P. C. B.; Carnell, A. J.; McKenzie, M. J. *Synlett* **1998**, 774–776.

(48) Hughes, D. L.; Smith, G. B.; Liu, J.; Dezeny, G. C.; Senanayake, C. H.; Larsen, R. D.; Verhoeven, T. R.; Reider, P. J. *J. Org. Chem.* **1997**, *62*, 2222–2229.

(49) Jacobsen, E. N.; Zhang, W.; Muci, A. R.; Ecker, J. R.; Deng, L. *J. Am. Chem. Soc.* **1991**, *113*, 7063–7064.

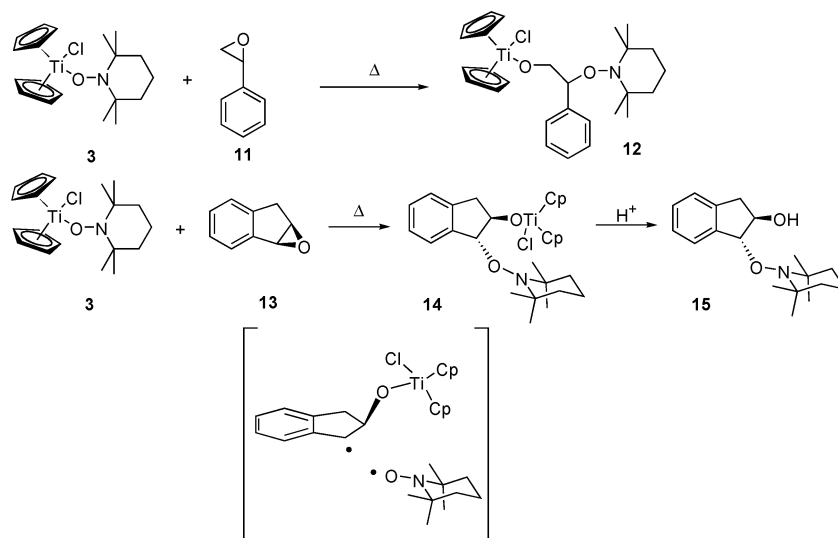


Figure 6. Epoxide opening with titanium TEMPO complex **3**.

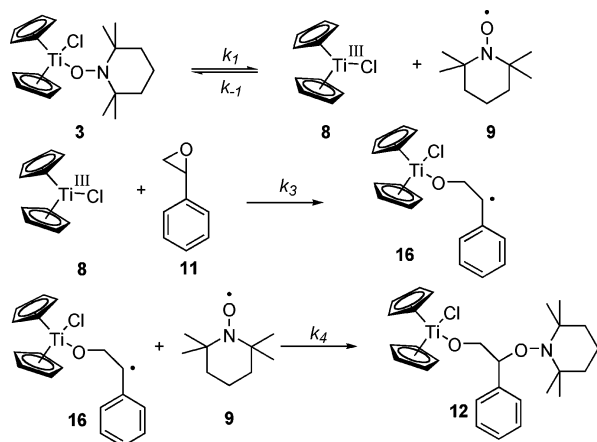


Figure 7. Kinetics of epoxide opening with titanium TEMPO complex **3**.

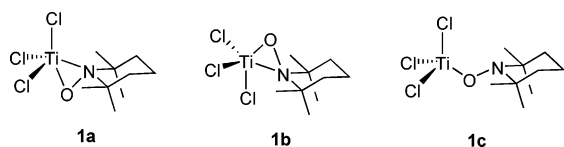


Figure 8. Calculated geometries for $\text{Cl}_3\text{Ti}(\text{TEMPO})$ **1**.

for complex **1** were calculated in order to locate global and local minima during geometry optimizations. For these calculations, a chair conformation for the piperidine ring was initially assumed and subsequently confirmed for the optimized geometries. For the η^2 geometries, the oxygen was placed at either the axial (**1a**) or the equatorial position (**1b**) of the TiCl_3 fragment and optimized to a locally stable geometry (Figure 8). The B3LYP/6-31G* geometry optimizations indicated that **1b** and **1c** are less stable than **1a** by 2 kcal/mol after ZPE correction. The identification of **1a** as the global minimum is consistent with the crystallographically determined structure for **1**.¹⁹ The slightly higher energy of **1b** is likely a consequence of the steric repulsion between the axial Cl atom and the two axial methyl groups of the piperidine ring as both **1a** and **1b** have similar core Ti–O–N bonding geometries. The DFT calculations reveal that the η^1 geometry in **1c** is only moderately higher in energy than the η^2 geometry in **1a**, which is consistent with solution measurements that indicate that the η^1 – η^2 inter-

conversion is facile at room temperature.²¹ For the η^1 structure of **1c**, the large Ti–O–N angle (164°) is similar to that found in $(\text{ArO})_2\text{TiCl}_2$ ⁶¹ and consistent with the contribution of p_π – d_π electron donation from oxygen to titanium (vide infra).^{28,57} However, the loss of the N–Ti coordination increases the energy of **1c** compared to **1a** and **1b**.

Geometry optimizations of metallocene **2** yielded geometrical parameters in good agreement with those from the crystal structure of **2**.¹⁹ The mean absolute difference of the five Ti–C, two Ti–Cl, two C–N, one Ti–O, and one N–O bond distances is 0.02 Å, providing further evidence that the B3LYP/6-31G* level of theory is appropriate to capture the key geometrical characteristics of these complexes (Table 3). Comparison of the structures of $\text{Cl}_3\text{Ti}(\text{TEMPO})$ **1** versus $\text{Cp}_2\text{TiCl}_2(\text{TEMPO})$ **2** reveals that the η^2 -coordination of the TEMPO ligand results in a lengthening of the Ti–O and N–O bonds of **1a** relative to that in **2**. For the η^1 -coordinated TEMPO in **1c**, these distances are more closely analogous to those of **2**. These results reveal that the Ti–O and Ti–Cl bonds of **1c** are slightly shorter than those of **2** (1.723 versus 1.753 Å for Ti–O bonds, 2.219 versus 2.279 Å for Ti–Cl bonds), implicating that the addition of a Cp ligand in **2** leads to lengthening of the Ti–Cl and Ti–O bonds and a decrease in the Ti–O–N bond angle (167.7 for **1c** versus 155.7° for **2**).^{26,28}

Structural Simulation of $\text{Cp}_2\text{TiCl}_2(\text{TEMPO})$ (3**) and the Effect of the Additional Cp.** As our experimental results had indicated that the Ti–O bonds for the bis(cyclopentadienyl) complexes **3** and **4** were weaker than that of the monocyclopentadienyl complex **2**,¹⁸ we were particularly interested in the influence of additional cyclopentadienyl ligands on the bonding geometries and energetics of Ti–O bonds. Geometry optimizations of **3** (Figure 9) reveal a N–O bond length of 1.426 Å and a Ti–O bond length of 1.842 Å, consistent with a covalent Ti–O bond to a reduced TEMPO ligand. Single-point energy calculations at the B3LYP/6-311G**/B3LYP/6-31G* level of theory show that the spin densities of Ti, O, and N atoms are all zero, consistent with this interpretation. Analysis of the bonding parameters reveals that the addition of the second cyclopentadienyl ligand has a significant influence on the Ti–O

(61) Waratuke, S. A.; Thorn, M. G.; Fanwick, P. E.; Rothwell, A. P.; Rothwell, I. P. *J. Am. Chem. Soc.* **1999**, *121*, 9111–9119.

Table 3. Selected Experimental and Calculated Bonds Lengths in 1–4^a

geometrical parameter	exp 1	calcd 1a	calcd 1c	geometrical parameter	exp 2	calcd 2	geometrical parameter	exp 4	calcd 4	calcd 3
Ti–O	1.838	1.842	1.723	Ti–O	1.753	1.758	Ti–O	1.824	1.845	1.842
Ti–N	2.112	2.151	-	Ti–N	-	-	Ti–N	-	-	-
Ti–Cl _a	2.258	2.272	2.215	Ti–Cl	2.279	2.279	Ti–Cl	2.534	2.400	2.404
Ti–Cl _e	2.218	2.220	2.219	Ti–Cp	2.015	2.056	Ti–Cp _a	2.028	2.106	2.107
N–O	1.433	1.416	1.392	N–O	1.412	1.403	N–O	1.406	1.420	1.426
N–C	1.527	1.535	1.502	N–C	1.502	1.505	N–C	1.536	1.500	1.506
Ti–O–N	79.4	81.5	167.7	Ti–O–N	155.7	154.3	Ti–O–N	145.6	144.5	144.8

^a Bond distances are reported in angstroms and angles in degrees.

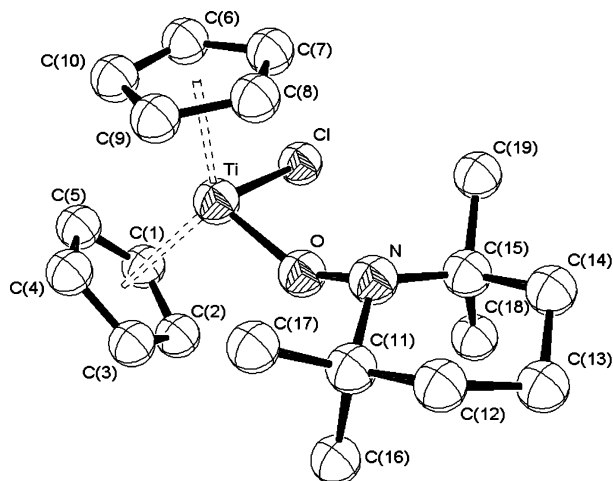


Figure 9. B3LYP/6-31G* optimized bond lengths (Å) and angles (deg) for **3**: Ti–Cp1, 2.214; Ti–Cp2, 2.107; Ti–O, 1.842; Ti–Cl, 2.404; N–O, 1.426; N–C11, 1.506; Cp1–Ti–Cp2, 128.8; Ti–O–N, 144.8; Cl–Ti–O, 97.0; O–N–C11, 107.5; O–N–C10, 109.1; C11–N–C15, 118.8.

and Ti–Cl bond lengths.²⁶ Comparison of the B3LYP/6-31G* optimized structure of **3** to that determined crystallographically for **2** reveals a significantly longer Ti–O bond distance of **3** relative to that of **2** (1.842 Å for **3** versus 1.753 Å for **2**) and a smaller Ti–O–N bond angle (144.8° in **3** versus 155.7° in **2**), as evidenced as well by the crystal structures of **4** versus **2** (Table 3).

Analysis of the molecular orbitals corresponding to Ti–O bonding reveals a combination of σ - and π -bonding for the Ti–O bonds. Presented in Figure 10 are the molecular orbitals corresponding to the Ti–O bonding interactions in **1c**, **2**, and **3** using an isodensity surface with a value of 0.03. For **1c** and **2**, a Ti–O σ -bond and two Ti–O π -bonds are clearly evident; similar multiple bonding between Ti and O was described for Cl₃TiOCH₃.⁵⁷ In contrast, for **3**, the molecular orbitals reveal a σ -bond (HOMO-39) and a π -bond (HOMO-11) in the Cl–Ti–O plane, but as π -bonding in the Cp–M–Cp plane is dominated by the strongly π -donating cyclopentadienyl ligands, the Ti–O π -interaction is diminished, analogous to the situation described for titanocene dithiolene complexes.⁶² Thus, analysis of the molecular orbitals suggests that there is less Ti–O π -bonding in the biscyclopentadienyl complex **2** relative to that in **3** as a consequence of the strong π -donor properties of the cyclopentadienyl ligand.

Calculated Ti–O Bond Energies. To assess the influence of the ancillary ligand environments on the strength of the Ti–O bonds, we carried out calculations on the bond dissociation

energies of the Ti–O bonds. Unless otherwise specified, all reported bond energies have been zero-point corrected and represent the energy at 0 K. In the cases of **3** and **4**, thermal corrections were also applied to obtain the enthalpy of the bond homolysis at 333.15 K in order to compare to experimental results. At the B3LYP/6-31G* level of theory, the calculated Ti–O bond dissociation energies were observed to depend sensitively on the ancillary ligation at Ti. For the Cl₃Ti(TEMPO) complexes **1a** and **1c**, the Ti–O bond is calculated to be 56 and 54 kcal/mol, respectively. This calculated bond energy is substantially weaker than that of typical Ti–O bonds (90 kcal/mol),²² as we had anticipated from the higher stability of the nitroxyl radical relative to typical alkoxy radicals. What we had not anticipated was the dramatic influence of the cyclopentadienyl ligands on the strength of these Ti–O bonds. Replacement of one of the chlorides with a cyclopentadienyl ligand to give compound **2** results in a weakening of the Ti–O bonds by approximately 11–13 kcal/mol (Table 4).

A more dramatic and unanticipated effect was observed on the addition of a second cyclopentadienyl ligand, as in **3**. The calculated bond energy of **2** is 43 kcal/mol, while those of **3** and **4** are both 17 kcal/mol, a difference of 26 kcal/mol! Comparison of the calculated (gas phase) bond energies, including thermal corrections to 333.15 K, with those derived from the nitroxyl exchange experiments for **3** and **4** (Table 4) reveals that the B3LYP/6-31G* level of theory leads to an underestimation of the bond energies if the experimental value is taken to be 25 kcal/mol. This 7–8 kcal/mol underestimation is similar to that observed from calculated and experimental estimates of the C–O bond strengths of alkoxyamines at this level of theory.^{60,63}

The significantly lower calculated Ti–O bond energy of **3** relative to that of **2** or **1** provides a rationale for our experimental observations that thermolysis of the biscyclopentadienyl complex **3** results in the homolytic cleavage of the Ti–O bond at 60 °C, whereas complex **2** is stable to homolytic cleavage at 100 °C for at least 24 h.¹⁸ As we were unable to measure the homolytic cleavage of the Ti–O bond in **2**, we have no experimental estimate for the strength of this bond; nevertheless, the fact that **2** is stable at 100 °C is consistent with the calculated difference of 26 kcal/mol.

Analysis of the structural parameters of **2** and **3** reveals that the lower Ti–O bond energies correlate to the longer Ti–O bonds of the geometry-optimized or crystallographically characterized complexes. The much lower bond energy of **3** relative to that of **2** or **1** might be attributed to both steric and electronic effects. Analysis of the nonbonded contacts between the

(62) Flemmig, B.; Strauch, P.; Reinhold, J. *Organometallics* **2003**, *22*, 1196–1202.

(63) Once more experiments become available, a higher level of theory might be warranted to obtain better agreement between experiment and theory.

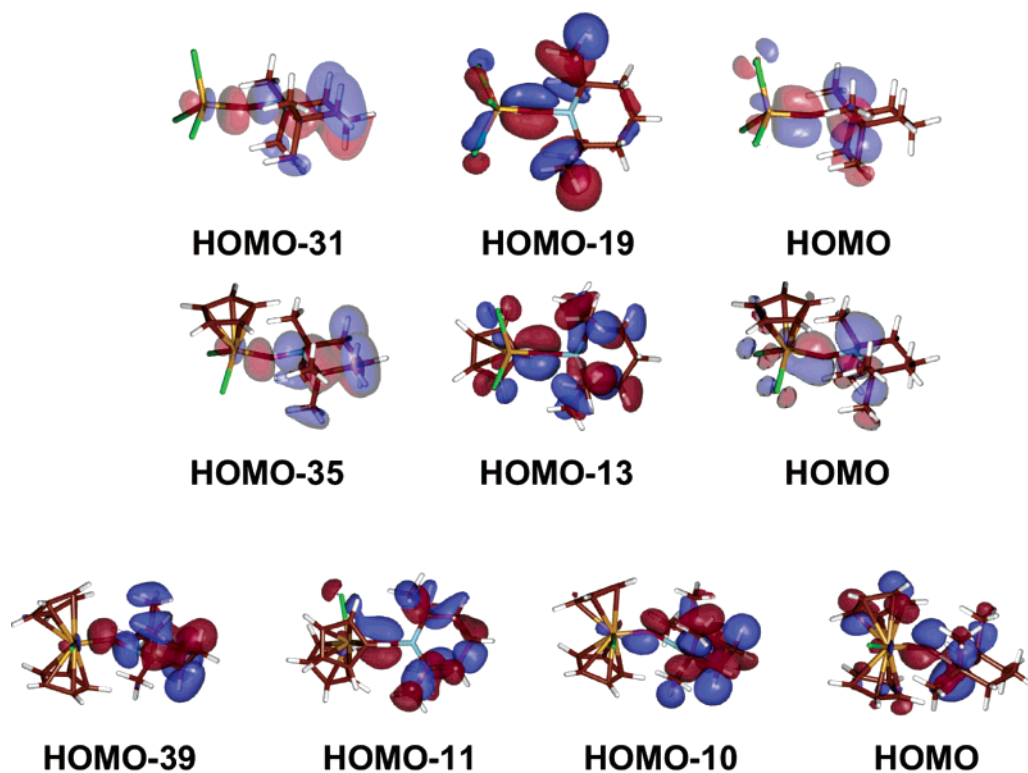


Figure 10. Isodensity plots of selected orbitals of **1c**, **2**, and **3** with a value of 0.03.

Table 4. Calculated Ti–O Bond Energies

	1a	1c	2	3	4	6	7
calcd Ti–O bond distance (Å)	1.842	1.723	1.758	1.842	1.845	1.862	1.769
Ti–O bond energy (kcal/mol) at 0 K (333.15 K)	56	54	43	17 (17)	17 (17)	30	50

hydrogen atom of the TEMPO methyl groups and those of the cyclopentadienyl ligands in **2** (2.780 Å) and **3** (2.229 Å) suggests that the sterically congested nature of **3** might contribute to a destabilization of the Ti–O bond. To assess the magnitude of these steric effects as well as to investigate the influence of the nature of the nitroxyl ligand on the Ti–O bond strength, we calculated the Ti–O bond energy of a less sterically hindered analogue **6**, where the TEMPO ligand is replaced by the 1-piperidinyloxy ligand (1-PO). The calculated Ti–O bond energy for **6** is 30 kcal/mol, 13 kcal/mol stronger than the Ti–O bond energy of **3**. This calculation reveals that the strength of Ti–O bonds derived from nitroxyl radicals also depends on the nature of nitroxyl ligand, as we observed experimentally from comparisons of **3** and **4** and as anticipated from analogous studies of the C–O bond of organic hydroxylamines.^{13,45} Comparison of the O–H bond strength of *N*-hydroxypiperidine (77.0 kcal/mol)⁶⁴ versus that of *N*-hydroxyltetramethylpiperidine (69.6 kcal/mol)^{65,66} reveals a difference of 7.4 kcal/mol in the O–H bond strengths. If the strength of the Ti–O bond correlates to the strength of the O–H bond of the hydroxylamines (not necessarily a good assumption), then we can get a crude estimate

of the steric contribution to the destabilization of the Ti–O bond energy of **3** of approximately 6 kcal/mol (that is, the Ti–O bond of **3** is approximately 6 kcal/mol weaker than we might predict on the basis of the relative strengths of the O–H bond of the corresponding hydroxylamines).

Another estimate of the steric destabilization of **3** can be calculated from the vertical bond (or snap) dissociation energies (vBDE) of **3** and **6**. This calculation involves a single-point energy calculation for the Cp₂TiCl and nitroxyl fragments upon cleavage of the Ti–O bond at the optimized geometry of the bound complexes. The geometries of the Cp₂TiCl and nitroxyl fragments are then optimized to get an estimate of the relaxation energies of the two fragments following the bond homolysis. To the extent that a component of the relaxation energy of the Cp₂TiCl fragment following bond homolysis represents the steric distortion of the Cp₂TiCl component in the bound complexes **3** and **6**, the differences in the relaxation energies provide an estimate of the steric effects on the Ti–O bond strengths.

These calculations reveal that the vBDEs for **3** and **6** are 52 and 60 kcal/mol, respectively. The relaxation energies of the Cp₂TiCl fragment derived from **3** and **6** are 18 and 14 kcal/mol, respectively, whereas the relaxation energies for the nitroxyl fragments are similar at 15 kcal/mol. This calculation reveals that the relaxation energy of the Cp₂TiCl fragment

(64) Bordwell, F. G.; Liu, W. Z. *J. Am. Chem. Soc.* **1996**, *118*, 8777–8781.

(65) Bordwell, F. G.; Liu, W. Z. *J. Am. Chem. Soc.* **1996**, *118*, 10819–10823.

(66) Mahoney, L. R.; Mendenha, G. D.; Ingold, K. U. *J. Am. Chem. Soc.* **1973**, *95*, 8610–8614.

derived from **3** is approximately 4 kcal/mol greater than that of **6**. This value is in reasonable agreement with the magnitude of the steric effect estimated from the difference in O–H bonds strengths.

A similar set of calculations involving the 1-PO analogue of **2**, CpTiCl₂(1-PO) (**7**), does not show the same steric effect. The ZPE-corrected bond dissociation energy increases from 43 kcal/mol in **2** to 50 kcal/mol in **7**. This difference of 7 kcal/mol is smaller than the change of 13 kcal/mol observed in the bis-Cp structures and is more closely in line with the differences in the O–H bond energies (7.4 kcal/mol). The vBDEs of **2** and **7** are 67 and 73 kcal/mol, respectively. The relaxation energies for the CpTiCl₂ fragment derived from **2** and **7** are both 11 kcal/mol, suggesting that there is very little steric effect contributing to the difference in Ti–O bond energies for the monocyclopentadienyl complexes **2** and **7**.

Comparison of these estimates reveals that steric effects are only partially responsible for extraordinarily weak Ti–O bond energy in **3** and cannot account for the 26 kcal/mol difference in the bond energies calculated for **2** and **3**. Moreover, comparison the Ti–O bond energies of the less sterically hindered analogues **6** and **7** shows a similarly large decrease in the Ti–O bond energy upon the addition of a second Cp ligand (the calculated bond energy of **6** is 20 kcal/mol weaker than that of **7**). This leads us to conclude that steric interactions between the cyclopentadienyl ligands and the TEMPO ligand are likely not the dominant effect that weakens the Ti–O bond in the biscyclopentadienyl complexes **3–6**, but rather the remarkable weakening of the Ti–O bond is due to an electronic effect of adding the strongly donating cyclopentadienyl ligand. One measure of this electronic effect can be obtained from the coefficients of the component atomic orbitals on the molecular bonding orbitals for the Ti–O bonds. For example, the coefficient of the oxygen p_z orbital (corresponding to the Ti–O σ-bond) changes from 0.154 to 0.136 to 0.100 for **1c**, **2**, and **3**, respectively.

The results of our experimental and theoretical studies indicate that the bond strengths of Ti–O bonds derived from the stable nitroxyl radical TEMPO are exquisitely sensitive to ancillary ligation environment. Calculations reveal that these Ti–O bonds weaken significantly upon substitution of chloride ancillary ligands with Cp ligands (Table 4, Cl₃Ti(TEMPO), **1c** = 54 kcal/mol; CpCl₂Ti(TEMPO), **2** = 43 kcal/mol; and Cp₂ClTi(TEMPO), **3** = 17 kcal/mol). These effects could be due to a destabilization of the Ti–O bonds by ancillary ligation or a preferential stabilization of the Ti(III) products by the cyclopentadienyl ligands. Both of these effects are likely to play a role, but our view is that the ability of cyclopentadienyl ligands to stabilize the highly coordinatively and electronically unsaturated Ti(III) species is likely a significant factor leading to the lower Ti–O bond energies. Are these observations specific to Ti–O bonds derived from nitroxyl radicals or representative of general bonding trends in early transition-metal systems? If the Cp effect is primarily a consequence of stabilizing the Ti(III) products, then these observations should be general to a variety of Ti–X bonds, but the evidence from the literature is not definitive on this question, due to the paucity of data on M–X bond strengths for a variety of ligation environments.^{22,67,68} Marks determined the Ti–I bond strengths for Cp^{tt}₂TiI₂ (40.6(5) kcal/mol) and Cp^{tt}₂TiI₂ (52.3(6) kcal/mol) (Cp^{tt} =

1,3-di-*tert*-butylcyclopentadienyl) and indicated that the value for Cp^{tt}₂TiI₂ was comparable to that of TiI₄ (56(2) kcal/mol).⁶⁷ The lower Ti–I bond energy of Cp^{tt}₂TiI₂ was attributed to steric effects. These data would suggest that the addition of Cp* ligands does not lead to a significant decrease in the Ti–I bond strengths, which is at variance with our observations for Ti–ONR₂ bonds. Nevertheless, it is known that Ti–Cl bond lengths increase upon substitution of chloride ancillary ligands with Cp ligands (av Ti–Cl: TiCl₄ = 2.163 Å,^{69,70} CpTiCl₃ = 2.22 Å,⁷¹ Cp₂TiCl₂ = 2.364 Å⁷²), and similar trends have been observed for Ti–OR bonds.^{23–26} Recent results from Ti and Cl K-edge X-ray absorption spectroscopy and DFT calculations reveal that the covalency of Ti–Cl bonds decreases in the series TiCl₄, CpTiCl₃, Cp₂TiCl₂, largely as a consequence of the strongly donating cyclopentadienyl ligand.⁷³ To the extent that longer bond lengths and lower covalencies correlate to weaker bonds, these trends would suggest that the influence of Cp ligands on the bonding of Ti–X bonds may not be unique to the nitroxyl-derived ligands, but representative of a more general trend in early transition-metal complexes. Further studies are warranted to test this hypothesis. Moreover, these results imply that the assumption of the transferability of Ti–X bond strengths among different ligand environments, which has proven to be useful in organometallic thermochemistry, should be re-examined, particularly for cyclopentadienyl ligands.^{22,67,68,74,75}

Conclusion

In conclusion, Ti–O bonds derived from stable nitroxyl radicals are considerably weaker than those of titanium alkoxides, and in appropriate ligation environments, they can be homolyzed at slightly elevated temperatures to generate Ti(III) complexes and nitroxyl radicals. The titanium(III) intermediates are rapidly trapped by nitroxyl radicals, but can competitively ring-open benzylic epoxides in high yield.

The strength of these Ti–O bonds is extremely sensitive to the ancillary ligation of titanium. Calculations at the B3LYP/6-31G* level of theory reveal that the addition of strongly donating cyclopentadienyl ligands results in a weakening of the Ti–O bond by up to 26 kcal/mol, providing a means of modulating the Ti–O bond energy over an interesting and experimentally accessible temperature range by appropriate manipulation of the ligand environment at titanium. The strong sensitivity of these Ti–O bonds to ancillary ligand environments implies that the influence of ancillary ligands, particularly cyclopentadienyl ligands, on Ti–X bond strengths is greater than previously anticipated.

Experimental Section

Computational Details. All of the quantum mechanical computations have been performed with the Gaussian 98 package⁵¹ using the all-electron 6-31G(d) basis set^{54–56} for all atoms at B3LYP level of theory.⁵² The exchange functional is a linear combination of Slater's

- (67) King, W. A.; Di Bella, S.; Gulino, A.; Lanza, G.; Fragala, I. L.; Stern, C. L.; Marks, T. J. *J. Am. Chem. Soc.* **1999**, *121*, 355–366.
- (68) Simoes, J. A. M.; Beachamp, J. L. *Chem. Rev.* **1990**, *90*, 629–688.
- (69) Morino, Y.; Uehara, H. *J. Chem. Phys.* **1966**, *45*, 4543–4550.
- (70) Troyanov, S. I.; Snigireva, E. M. *Russ. J. Inorg. Chem.* **2000**, *45*, 580–585.
- (71) Engelhardt, L. M.; Papasergio, R. I.; Raston, C. L.; White, A. H. *Organometallics* **1984**, *3*, 18–20.
- (72) Clearfield, A.; Warner, D. K.; Saldarriagamolina, C. H.; Ropal, R.; Bernal, I. *Can. J. Chem. Rev. Can. Chim.* **1975**, *53*, 1622–1629.
- (73) Debeer, G. S.; Brant, P.; Solomon, E. I. *J. Am. Chem. Soc.* **2005**, *127*, 667–674.

local spin density, Becke's 1988 nonlocal, and exact (Hartree–Fock) exchange terms. The correlation functional is a combination of Lee–Yang–Parr and VWN local spin density correlation functionals.⁵³ Geometry optimizations of all the structures were performed using the default convergence criteria without any geometric constraints. Frequency calculations were performed to confirm that geometries were at the minimum of an energy well. The unscaled frequencies obtained from these calculations were also used to determine the zero-point energies (ZPE) as well as thermal corrections when applicable. The thermal corrections included translation, rotational, vibrational, and electronic contributions to the partition function. All internal rotations were treated using a harmonic oscillator approximation.

General Considerations. Nitrogen gloveboxes and standard Schlenk techniques were applied in handling all oxygen and moisture-sensitive compounds. Pentane and toluene were purchased from Aldrich and purified through towers containing alumina and Q5 prior to use. Tetrahydrofuran and *d*₆-benzene were vacuum transferred from purple sodium/benzophenone solutions. Styrene oxide obtained from Aldrich was dried over CaH₂ and distilled in vacuo prior to use. Cp₂TiCl₂ was obtained from Strem Chemicals, Inc. and used without further purifications. TEMPO and 4-MeO-TEMPO were purchased from Aldrich and sublimed in vacuo prior to use. Zinc dust was purchased from Aldrich, dried in vacuo overnight, and stored under N₂ prior to use. Cp* CpTiCl₂⁴⁶ and indene oxide⁷⁶ were synthesized according to the literature procedures.

¹H NMR spectra were recorded at 400 MHz on a Varian Mercury 400. ¹³C NMR spectra were recorded at 100 MHz on the same instrument. The temperatures of the probe for variable temperature studies were calibrated by ethylene glycol. ¹H and ¹³C chemical shifts were referenced relative to tetramethylsilane by internal residual solvent peaks. Elemental analyses were carried out at either Desert Analytics Laboratory (Arizona, USA) or Atlantic Microlab, Inc. (Georgia, USA). High-resolution mass spectra (HRMS) were performed on a Micromass Q-ToF hybrid quadrupole-time-of-flight LC-MS in the Vincent Coates Foundation Mass Spectrometry Laboratory at Stanford University.

Synthesis of Cp₂TiCl(4-MeO-TEMPO) (4) and Cp* CpTiCl(TEMPO) (5). Complex 4: To a mixture of Cp₂TiCl₂ (747 mg, 3 mmol) and Zn (451 mg) was added 30 mL of THF. This mixture was stirred for 30 min. This green mixture was then filtered to remove excess Zn. A solution of 558 mg of 4-MeO-TEMPO (3 mmol) in 10 mL of THF was cannulated into the filtrate. After stirring for 5 h, THF was removed in vacuo. The residue was extracted with 40 mL of toluene. The resulting solution was filtered to remove ZnCl₂. Toluene was removed in vacuo and the residue extracted with 100 mL of pentane. The resulting brown solution was filtered. Brown–red thin plates were obtained after recrystallization from the pentane filtrate (666 mg, 55.5%). ¹H NMR (C₆D₆, 60 °C): δ 1.01 (s, 6H), 1.28 (s, 6H), 1.54 (m, 2H), 1.83 (m, 2H), 3.13 (s, 3H), 3.26 (m, 1H), 6.07 (s, 10H). ¹³C NMR (C₆D₆, 60 °C): δ 117.1, 71.5, 63.0, 55.4, 46.1, 32.5 (b), 22.7 (b). Anal. Calcd: C, 60.09; H, 7.56; N, 3.50. Found: C, 60.27; H, 7.82; N, 3.65.

Complex 5: This was prepared from Cp* CpTiCl₂ and TEMPO using the same procedure as for **4** but on a smaller scale (1 mmol). Brown–red needles were obtained after recrystallization twice from the pentane (140 mg, 31.9%). ¹H NMR (C₆D₆, 60 °C): δ 1.07 (s, 6H), 1.28 (s, 3H), 1.36–1.62 (m, 6H), 1.15 (s, 3H), 1.85 (s, 15H), 6.15 (s, 5H). ¹³C NMR (C₆D₆, 60 °C): δ 125.4, 118.1, 64.3, 61.2, 43.3, 42.1, 33.7, 32.0, 22.7, 22.1, 17.1, 13.1. Anal. Calcd: C, 65.53; H, 8.71; N, 3.18. Found: C, 65.45; H, 8.81; N, 3.04.

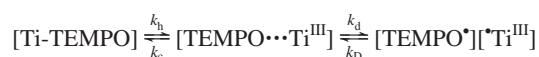
Thermolysis of Cp₂TiCl(TEMPO) (2) in the Presence of 4-MeO-TEMPO (10). To 3.7 mg of Cp₂TiCl(TEMPO) ([2]₀ = 1.0 × 10^{−2} M) and a few crystals of hexamethylbenzene (used as the internal standard)

in 1.0 mL of *d*₆-benzene solution were added various amounts of 4-MeO-TEMPO (18.6–46.5 mg) (Table 1). These reactions were monitored by ¹H NMR on a Varian Mercury 400 at 40–65 °C. The ratio of ([2]_t/[2]₀) was determined by the integration of the Cp proton signal of Cp₂TiCl(TEMPO)/the sum of the integration of the Cp proton signals in both Cp₂TiCl(TEMPO) and Cp₂TiCl(4-MeO-TEMPO) using gNMR³¹ analysis, assuming a 10% error for NMR integrations.

Thermolysis of Cp₂TiCl(MeO-TEMPO) (4) in the Presence of TEMPO (9). Cp₂TiCl(4-MeO-TEMPO) (4.0 mg) ([4]₀ = 1.0 × 10^{−2} M), TEMPO (31.2 mg), and a few crystals of hexamethylbenzene (used as the internal standard) were dissolved in 1.0 mL of *d*₆-benzene solution. These reactions were monitored by ¹H NMR on a Varian Mercury 400 at 40–65 °C.

Thermolysis of Cp* CpTiCl(TEMPO) (5) in the Presence of 4-MeO-TEMPO (10). Cp* CpTiCl(TEMPO) (4.4 mg) ([5]₀ = 1.0 × 10^{−2} M), TEMPO (37.2 mg), and a few crystals of hexamethylbenzene (used as the internal standard) were dissolved in 1.0 mL of *d*₆-benzene solution. These reactions were monitored by ¹H NMR on a Varian Mercury 400 at 25–50 °C.

Estimation of the Cage Effect.



Koenig and Finke have discussed the importance of radical cage effects in detail.³⁷ If the cage effect is important, *k*₁ (*k*_{obs}) and *k*_{−1} should be referred to as (*k*_d*k*_h/(*k*_c + *k*_D)) and (*k*_c*k*_D/(*k*_c + *k*_D)), respectively, where the fractional cage efficiency *F*_c = *k*_c/(*k*_c + *k*_D). The bond dissociation energy³⁷

$$\text{BDE} \approx \Delta H_{\text{obs}}^{\ddagger}(\text{soln}) + (1 - F_c)[\Delta H_{\text{d}}^{\ddagger} - \Delta H_{\text{c}}^{\ddagger}] - \Delta H_{-1}^{\ddagger}(\text{soln})$$

where Δ*H*_d[‡] is the enthalpy of escape from the cage, Δ*H*_c[‡] the radical recombination enthalpy, Δ*H*_{−1}[‡](soln) the enthalpy of formation of the cage, and *F*_c is defined above. If we assume that *F*_c = 1, that solvation of the various transition states are similar (δ (solvation) = 0), and that Δ*H*_{−1}[‡](soln) ≈ 1.9 kcal/mol (the activation enthalpy for a diffusion-controlled reaction in benzene),⁴⁰ then we can calculate an upper limit of the Ti–O BDE of **3** ≈ Δ*H*_{obs}[‡](soln) − Δ*H*_{−1}[‡](soln) = 27(±1) − 1.9 = 25(±1) kcal/mol, or approximately 25 kcal/mol.

Synthesis of 12: Cp₂TiCl(TEMPO) (370 mg, 1 mmol) and styrene oxide (240 mg, 2 mmol) were dissolved in 10 mL of toluene in a reaction tube. The reaction mixture was heated at 125 °C for 10 min and cooled to room temperature. Then, 15 mL of pentane was added into the mixture. The product was recrystallized twice at −50 °C to give a pale yellow solid (345 mg, 72%). ¹H NMR (C₆D₆): δ 0.86 (s, 3H), 1.11 (s, 3H), 1.29 (s, 3H), 1.50 (s, 3H), 1.20–1.50 (bm, 6H), 4.71 (dd, *J* = 7.2, 11.6 Hz, 1H), 4.81 (dd, *J* = 4.4, 7.2 Hz, 1H), 5.02 (dd, *J* = 4.4, 11.6 Hz, 1H), 5.73 (s, 5H), 5.84 (s, 5H), 7.11 (t, *J* = 7.6 Hz, 1H), 7.21 (t, *J* = 7.6 Hz, 1H), 7.34 (t, *J* = 7.6 Hz, 1H). ¹³C NMR (C₆D₆): δ 143.3, 128.3, 127.9, 127.3, 116.3, 87.5, 84.9, 60.1, 40.7, 34.5, 20.6, 17.5. Anal. Calcd: C, 66.19; H, 7.41; N, 2.86. Found: C, 66.13; H, 7.37; N, 2.72.

Reaction of (3) with Indene Oxide (13): Cp₂TiCl(TEMPO) (20.7 mg, 0.056 mmol) and indene oxide (7.4 mg, 0.056 mmol) were dissolved in 0.7 mL of *d*₆-benzene in a J-Young tube. The reaction was heated at 100 °C for 5 min. From the quantitative yield by ¹H NMR, only one product was observed, >99% trans selectivity as confirmed by ROESY. ¹H NMR (C₆D₆): δ 1.00 (s, 3H), 1.20 (s, 6H), 1.39 (s, 3H), 1.13–1.52 (bm, 6H), 2.94 (dd, *J* = 3.0, 16.8 Hz, 1H), 3.26 (dd, *J* = 6.0, 16.8 Hz, 1H), 5.27 (d, *J* = 3.0 Hz, 1H), 5.50 (ddd, *J* = 3.0, 3.0, 6.0 Hz, 1H), 5.94 (s, 5H), 5.98 (s, 5H), 7.08–7.13 (m, 3H), 7.67 (dd, *J* = 1.6, 7.2 Hz, 1H). ¹³C{¹H} NMR (C₆D₆): δ 143.1, 141.6, 128.8, 127.6, 126.2, 125.2, 116.6, 116.1, 96.1, 92.8, 60.5, 60.1, 40.7, 40.5, 39.7, 34.4, 33.9, 20.7 (br), 17.6.

Isolation of (15): The *d*₆-benzene solution of **14** was diluted with 2 mL of diethyl ether. This solution was mixed with 2 mL of 0.5 M HCl

(74) Schock, L. E.; Marks, T. J. *J. Am. Chem. Soc.* **1988**, *110*, 7701–7715.

(75) Marks, T. J. *Bonding Energetics in Organometallic Compounds*; American Chemical Society: Washington D.C., 1990; Vol. 428.

(76) Imuta, M.; Ziffer, H. *J. Org. Chem.* **1979**, *44*, 1351–1352.

(aq). The organic layer was separated. The aqueous layer was extracted with 3×1 mL of ether. The organic layers were combined, washed with brine (2×2 mL), and dried over Na_2SO_4 . Then the solution was eluted through a silica gel column. Solvent was removed in vacuo to give **15** as a pale yellow oil (15.2 mg, 94%). ^1H NMR (CDCl_3): δ 1.13 (s, 3H), 1.29 (s, 6H), 1.30 (s, 3H), 1.32–1.56 (m, 6H), 2.76 (dd, $J = 8.4, 14.8$ Hz, 1H), 3.16 (dd, $J = 7.2, 14.8$ Hz, 1H), 3.45 (br, 1H), 4.71 (dt, $J = 8.4, 7.2$ Hz, 1H), 5.35 (d, $J = 7.2$ Hz, 1H), 7.16–7.23 (m, 3H), 7.37 (m, 1H). $^{13}\text{C}\{^1\text{H}\}$ NMR (CDCl_3): δ 140.2, 138.4, 127.9, 126.6, 124.8, 124.1, 90.2, 79.9, 61.6, 59.7, 40.4, 40.2, 36.9, 34.7, 33.7, 20.4 (2C), 17.2. HRMS Calcd for $\text{C}_{18}\text{H}_{28}\text{NO}_2$ ($M + 1$ for $[\text{M} + \text{H}]^+$): 290.2120. Found: 290.2112.

Thermolysis of $\text{Cp}_2\text{TiCl}(\text{TEMPO})$ (3**) in the Presence of an Excess Amount of Styrene Oxide (**11**):** $\text{Cp}_2\text{TiCl}(\text{TEMPO})$ (4.5 mg, 0.012 mmol), styrene oxide (29.3 mg, 0.244 mmol), and a few crystals of hexamethylbenzene (used as the internal standard) were dissolved in 1.0 mL of d_6 -benzene. The reaction was monitored by ^1H NMR on a Varian Mercury 400 at 60 °C. The ratio of $[\mathbf{3}]/[\mathbf{3}]_0$ was determined by the integration of the Cp proton signal of **3**/the sum of the integration of the Cp proton signals in both **3** and **12**, assuming a 10% error for NMR integrations.

X-ray Data Collection and Reduction. Full details are contained in the Supporting Information. A colorless rhombic crystal of $\text{Cp}_2\text{TiCl}(\text{MeO-TEMPO})$ (**4**) having approximate dimensions of $0.44 \times 0.25 \times 0.04$ mm³ was mounted on a quartz fiber using Paratone N hydrocarbon oil. All measurements were made on a Bruker-Siemens SMART⁷⁷ CCD area detector with graphite monochromated Mo $K\alpha$ radiation ($\lambda = 0.71073$ Å). Data were integrated by the program SAINT with box parameters of $1.0 \times 1.0 \times 0.6^\circ$. Of the 9114 reflections which were collected, 3308 were unique ($R_{\text{int}} = 0.070$). No decay correction was applied. The structure was solved by direct methods⁷⁸ and expanded using Fourier technique.⁷⁹ The non-hydrogen atoms were refined

(77) *Smart*, Area-Detector Software Package; S. I. A., Inc.: Madison, WI, 1995.

(78) Sheldrick, G. M. *SHELXS97: A Program for Crystal Structure Refinement*; University of Göttingen: Göttingen, Germany, 1997.

anisotropically. Hydrogen atoms were located by difference Fourier synthesis and were constrained to idealized geometries in a riding (AFIX) refinement. A single free rotation angle about the C–CH₃ bond vector was also refined in the case of methyl groups. Scattering factors were taken from the International Tables for Crystallography.⁸⁰ All calculations were performed using the CrystalStructure^{81,82} crystallographic software package, except for refinement, which was performed using SHELXL-97.⁷⁸

Acknowledgment. We acknowledge the financial support from the National Science Foundation (NSF-CHE 0097839). We are indebted to Wei-Chen Chen at Caltech, Abhishek Dey at Stanford, and Yuan-Chung Cheng and Kan-Lian Hu at MIT for useful discussions. K.-W.H. acknowledges a Regina Casper Stanford Graduate Fellowship. J.H.H. acknowledges an NSF Graduate Fellowship. This paper is dedicated to the memory of Mr. Chao-Chun Huang and Mrs. Yu-Mei Lin-Liu; and to Professor Henry Taube on the occasion of his 90th birthday.

Supporting Information Available: Cartesian coordinates for the calculated structures of **1a–c**, **2–4**, **6**, and **7** at B3LYP/6-31G*, synthesis, characterization, and X-ray crystallographic data of **4**, figures and tables giving a summary of kinetic data. This material is available free of charge via the Internet at <http://pubs.acs.org>.

JA044512F

(79) Beurskens, P. T.; Admiraal, G.; Beurskens, G.; Bosman, W. P.; de Gelder, R.; Israel, R.; Smits, J. M. M. *DIRDIF99*; The DIRDIF-99 Program System, Technical Report of the Crystallography Laboratory, University of Nijmegen: The Netherlands, 1999.

(80) *International Tables for Crystallography*, Vol. C.; Kluwer Academic Publishers: Dordrecht, The Netherlands, 1992; Tables 4.2.6.8 and 6.1.1.4.

(81) *CrystalStructure 2.00*: Crystal Structure Analysis Package, Rigaku and MSC, 2001.

(82) Watkin, D. J.; Prout, C. K.; Carruthers, J. R.; Betteridge, P. W. *CRYSTALS Issue 10*; Chemical Crystallography Laboratory: Oxford, U.K.